ORIGINAL ARTICLE

LncRNA BASP1-AS1 interacts with YBX1 to regulate Notch transcription and drives the malignancy of melanoma

YaLing Li[1] | YaLi Gao[2] | XueLi Niu[1] | MingSui Tang[1] | JingYi Li[1] | Bing Song[1,3] | XiuHao Guan[1] iD

[1]Department of Dermatology, The First Hospital of China Medical University and National Joint Engineering Research Center for Theranostics of Immunological Skin Diseases, The First Hospital of China Medical University and Key Laboratory of Immunodermatology, Ministry of Health and Ministry of Education, Shenyang, China

[2]Department of Dermatology, The First Affliacted Hospital of Sun Yat-sen University, Guangzhou, China

[3]School of Dentistry, Cardiff University, Cardiff, UK

Correspondence
Bing Song, School of Dentistry, Cardiff University, Heath Park, Cardiff, CF14 4XY, UK.
Email: SongB3@cardiff.ac.uk

Xiu-Hao Guan, Department of Dermatology, Key Laboratory of Immunodermatology, No.155 Nanjing North Street, Heping District, 110001 Shenyang, Liaoning Province, China.
Email: cmugxh@126.com

Funding information
National Science Fundation of China-Liaoning Joint Programme, Grant/Award Number: U1908206

Abstract

Melanoma is a fatal skin malignant tumor with a poor prognosis. We found that long noncoding RNA *BASP1-AS1* is essential for the development and prognosis of melanoma. The methylation, RNA sequencing, copy number variation, mutation data, and sample follow-up information of melanoma from The Cancer Genome Atlas (TCGA) were analyzed using weighted gene co-expression network analysis and 366 samples common to the three omics were selected for multigroup clustering analysis. A four-gene prognostic model (*BASP1-AS1*, *LOC100506098*, *ARHGAP27P1*, and *LINC01532*) was constructed in the TCGA cohort and validated using the GSE65904 series. The expression of *BASP1-AS1* was upregulated in melanoma tissues and various melanoma cell lines. Functionally, the ectopic expression of *BASP1-AS1* promoted cell proliferation, migration, and invasion in both A375 and SK-MEL-2 cells. Mechanically, *BASP1-AS1* interacted with YBX1 and recruited it to the promoter of NOTCH3, initiating its transcription process. The activation of the Notch signaling then resulted in the transcription of multiple oncogenes, including c-MYC, PCNA, and CDK4, which contributed to melanoma progression. Thus, *BASP1-AS1* could act as a potential biomarker for cutaneous malignant melanoma.

KEYWORDS
BASP1-AS1, melanoma, NOTCH3, signature, YBX1

1 | INTRODUCTION

Melanoma is a malignant tumor caused by melanocytes,[1] and its incidence has been increasing in recent years. Despite the development and application of more treatments,[2,3] the prognosis of melanoma remains poor,[4,5] therefore finding new molecules and developing new biomarkers are needed to improve the prognosis of melanoma patients.

Long noncoding RNAs (LncRNAs) are defined as RNAs of more than 200 nucleotides in length with limited protein-coding capacity,[6] in fact, it has been suggested that LncRNAs are involved with many biological processes, and their key role in cell and tumor specificity

indicates their potential for use as diagnostic markers or therapeutic targets in many cancer types.[7] LncRNAs regulate various oncogenes and tumor suppressor genes at the transcriptional, translational, protein localization, and functional levels; moreover, they are also involved in the epigenetic regulation of cell cycles, differentiation, apoptosis, DNA repair, and metabolism.[8-10]

With the maturity of high-throughput sequencing technology, large-scale omics data generation is allowed.[11,12] However, differential expression analysis only considers each gene without considering the relationship between genes. Therefore, trying to explain the complex relationship between genes is still challenging.[13,14] Nevertheless, the application of network analysis using a WGCNA has advantages in describing and analyzing molecular mechanisms and network relationships.[15] Furthermore, WGCNA has achieved a series of results in melanoma research.[16-18]

In this work, the methylation, RNA-Seq, CNV, mutation data, and sample follow-up information of melanoma from TCGA were analyzed using WGCNA. We used prognostic-related coding genes, CNV, and methylation sites, and selected 366 samples shared by the three omics to conduct a multigroup clustering analysis to construct a prognostic model of four genes in the TCGA cohort, which was verified by GSE65904. Survival analysis showed that functional LncRNAs-CNV might be a candidate prognostic biomarker for clinical application, and *BASP1-AS1* is a new LncRNA that has not been screened out in melanoma, even if it has been found that *BASP1-AS1* regulates *BASP1* in HNPCs and plays a key role in neuronal differentiation.[19]

YBX1 (Y box binding protein 1) is an RNA/DNA binding multifunctional protein, which is recognized as a carcinogenic transcription factor that can regulate apoptosis, translation, cell proliferation, mRNA splicing, repair, differentiation, and the stress response.[20] Additionally, studies have shown that the LncRNA *DSCAM-AS1* interacts with YBX1 to promote cancer progression by forming a positive feedback loop that activates the FOXA1 transcription network.[21] Non-coding RNA *HOXC-AS3* mediates the occurrence of gastric cancer by binding to YBX1.[22] However, both the regulation and mechanism of action of YBX1 in melanoma remain unclear, limiting the discovery of its potential therapeutic strategies. In addition, c-MYC is a proto-oncogene that can induce cell transformation and regulate programmed cell death. A large number of studies have shown that c-MYC overexpression can promote the development of melanoma.[23,24]

In this study, the methylation, RNASeq, CNV, mutation data, and follow-up information of melanoma in TCGA were analyzed for multigroup clustering analysis. It was found that the expression of LncRNA *BASP1-AS1* in melanoma tissue was increased and that it was related to the clinical outcome of melanoma patients. Functionally, the ectopic expression of *BASP1-AS1* promoted cell proliferation, migration, and invasion in both A375 and SK-MEL-2 cells. Mechanically, *BASP1-AS1* interacted with YBX1 and recruited it to the promoter of NOTCH3, initiating its transcription process. The activation of the Notch signaling then resulted in the transcription of multiple oncogenes, including *c-MYC*, PCNA, and CDK4, which contributed to melanoma progression. These results suggest that *BASP1-AS1* plays an important role in the progression and prognosis of melanoma, and can be used as a potential diagnostic and prognostic biomarker.

2 | MATERIALS AND METHODS

2.1 | Patients and tissues

A total of 15 melanoma samples and matched nontumorous tissue were obtained from the First Hospital of China Medical University, all enrolled patients provided written informed consent, and this study was approved by the Ethics Committee of the First Hospital of China Medical University. For qRT-PCR detection, cutaneous melanoma tissues were obtained, snap-frozen in liquid nitrogen, and stored at −80°C after surgery.

2.2 | Data analysis

Methylation, RNA-Seq, CNV, mutation data, and follow-up information of melanoma samples were downloaded from the TCGA GDC. We selected the samples with a follow-up time of more than 30 days and used the univariate COX proportional hazard regression to establish the model. Next, the common samples of the three omics were selected, and the R software package iClusterPlus was used for multigroup clustering analysis. We further analyzed the differential LncRNAs and encoding genes in different subtypes. Using the R software package DEseq2, we first removed the genes with an average number of counts less than 1 from the expression profile and further used foldchange greater than 2 and fdr < 0.05 as the threshold to screen the differential LncRNAs and encoding genes in different subtypes. Furthermore, we use the absolute value of the difference multiple as rank to do a GSEA analysis according to the different multiples of LncRNA in each subtype. Afterward, a Pearson correlation coefficient was used to calculate the distance between each gene and the LncRNA, and the R software package WGCNA was used to construct the weight co-expression network. Further analysis of the function of these modules was done using the R software package clusterProfiler for KEGG pathway enrichment analysis. Afterwards, the proportion of multicopy and copy deletion of each LncRNA was counted, and its distribution was observed in the genome.

To systematically identify LncRNA prognostic markers, we analyzed the copy number of LncRNAs that were different in each subtype and selected LncRNAs that had a copy number change rate of more than 0.1% in each sample and at least one difference in each subtype, and the copy number was positively correlated with the expression level. Univariate survival analysis was used to analyze the relationship between LncRNAs and total survival time. According to the expression of LncRNAs, the samples were divided into high and low expression groups, with the top 25% as the high expression group and the lowest 25% as the low expression group. The KM method was used to analyze the difference between the two groups. Multivariate survival analysis was used to observe whether these LncRNAs were

independent prognostic factors. We then used stepwise multivariate regression to screen independent prognostic factors.

2.3 | Cell culture and transfection

All cell lines were obtained from the Chinese Academy of Sciences and were cultured in DMEM supplemented with 10% fetal bovine serum (FBS; Gibco) and 1% penicillin-streptomycin in an incubator with humidified 5% CO_2 at 37℃. At 24 hours before transfection, A375 and SK-MEL-2 cells were planted in six-well plates with 50-60% confluence and then transfected with siRNA by using Lipofectamine 2000 according to the manufacturer's instructions.

2.4 | RNA isolation and qRT-PCR

Briefly, total RNA was isolated from tissues and cells by using TRIzol® reagent (Thermo Fisher Scientific, Inc) and then reverse-transcribed using QuantiTect Reverse Transcription Kit (Qiagen) according to the manufacturer's specifications. Quantitative real-time PCR (qRT-PCR) amplification was performed using SYBR-Green PCR mix (Takara) and the expression levels of target genes were normalized to the level of GAPDH or U6.

2.5 | Cell colony formation assay

Cell colony formation assay was performed as previously described.[25]

2.6 | Cell migration and invasion assay

A375 and SK-MEL-2 cells migration and invasion assay was performed as previously described.[25]

2.7 | RNA pull-down assay

The biotin-coupled RNA complex was pulled down by incubating the melanoma cell lysates with streptavidin-coated magnetic beads (Sigma) following the manufacturer's instructions. qRT-PCR analysis was used to evaluate the enrichment of BASP1-AS1 in the captured fractions. Both the BASP1-AS1 junction probe and the control probe were obtained from Sangon Biotech. The proteins in the capture complex were identified by western blotting using an anti-YBX1 antibody.

2.8 | ChIP assay

Chromatin immunoprecipitation (ChIP) assay was performed using a High-Sensitivity ChIP Kit (Abcam) according to the manufacturer's specifications. In brief, cells were fixed with 4% paraformaldehyde

and incubated with glycine for 20 min to enhance DNA-protein cross-links. Then cells were lysed, and DNA was sonicated to generate chromatin fragments of 400-800 bp. After sonication, the DNA fragments were immunoprecipitated with Magnetic Protein A Beads conjugated with YBX1 antibody (Abcam) or rabbit nonimmune IgG (as negative control) overnight. The next day, the precipitated DNA was analyzed by PCR with NOTCH3 promoter-specific primers.

2.9 | RIP assay

The RNA immunoprecipitation (RIP) experiment was performed using a Magna RIPTM RNA Binding Protein Immunoprecipitation Kit (Millipore) according to the manufacturer's specifications. In brief, cells were lysed in RIPA buffer containing both a protease inhibitor cocktail and an RNase inhibitor, and then incubated with buffer containing magnetic beads conjugated with 5 μg human anti-YBX1 antibody or immunoglobulin G (IgG) control at 4℃ for 6 h. Afterwards, the beads were incubated with proteinase K to digest proteins. Finally, purified RNA was analyzed with RT-PCR for further study.

2.10 | Western blot assay

Cells were lysed using RIPA Lysis containing Protease/Phosphatase Inhibitor Cocktail (Abcam). The extracted proteins were separated in 10% SDS-polyacrylamide gel and then transferred to immobilon-P membranes (Merck Millipore). The membrane was blocked with 5% nonfat dry milk in PBS containing 0.1% Tween 20 (PBST) for 1 h at room temperature and then incubated with primary antibodies at 4℃ overnight. The next day, the membranes were washed three times with Tris-buffered saline Tween and then incubated with HRP-conjugated secondary antibody (1:1000, Santa Cruz Biotech) for 2 h at room temperature. Finally, all bands were detected using ECL Western blotting kit (Amersham Biosciences). GAPDH was used as an internal reference.

2.11 | Xenografts assays

Four-week-old athymic male BALB/c nude mice were purchased and randomly divided into different groups. Then, 2×10^6 cells were inoculated subcutaneously in the right flank of the nude mice. Five weeks after cell inoculation, the mice were sacrificed and the tumors were collected. The protocol of animal experiments was approved by the Institutional Animal Care and Use Committee of the First Hospital of China Medical University. The animal experiments were conducted based on minimized animal number and the least pains on experimental animals.

2.12 | Statistical analysis

Statistical analysis was performed using SPSS 18.0 software and Graphpad Prism 7 was used as the mapping software. The data were

presented as the mean ± SD as indicated. Comparison between two groups was assessed using an unpaired two-tailed *t*-test, with $P < .05$ being considered as statistically significant.

3 | RESULTS

3.1 | Multiomics screening of LncRNA differences in melanoma subtypes

We screened 3509 coding genes from TCGA GDC and 2199 CNV regions, and 25 788 CpG sites. We used prognosis-related coding genes, CNV, methylation sites, and selected a total of 366 samples from three omics, and conducted multi-omics cluster analysis. The number of classifications was five, and five subtypes were obtained (Table 1). The distribution of mRNA expression level, CNV, and methylation in each subtype can be seen in Figure 1A, from which it can be seen that there are differences in the three distribution levels among each subtype. Furthermore, we analyzed the prognosis differences of these five subtypes (Figure 1B), and these five subtypes had prognosis differences ($P < .0001$), with the prognosis of group C1 being the worst. At the same time, we counted the proportion of gene mutations in different subtypes and selected the 20 genes with the highest proportion of mutations in each subtype, and a total of 44 genes were obtained. The intersection of the 20 genes with the highest frequency of mutation in the five subtypes samples is shown in Figure 1C, which suggests that the coincidence degree between the genes with the highest frequency of mutation between the five subtypes is high.

Furthermore, we show the mutations of these 44 genes in each subtype in Figure 1D. Further screening and analysis of different subtypes of LncRNA and coding genes were done and the differences of each subtype are summarized in Table 2. A total of 3807 differential LncRNAs (All.DElncRNA.txt) and 5057 encoding genes were obtained. The differential volcanic maps of LncRNAs in each subtype are shown in Figure 1E-I. The number of LncRNA differences and the number of gene differences in each subtype were counted as shown in Figure 1J. Moreover, we downloaded LncRNAs closely related to melanoma from the LncRNADisease and Lnc2Cancer database, and a total of 180 LncRNAs (disease.lncRNA.txt) were obtained, which were compared with 3807 differential LncRNAs, as shown in Figure 1K. There were 90 LncRNAs closely related to disease (disease.DElncRNA.txt), and the significance was tested by hypergeometric test ($P < .001$).

TABLE 1 Number of samples of five subtypes

Cluster	Sample count
C1	39
C2	57
C3	142
C4	16
C5	112

As shown in Figure S1A-E, the results of GSEA analysis showed that differentially expressed LncRNAs were clustered, with large differences between the gene clusters. We analyzed the intersection of LncRNAs between five subtypes and cancer and normal samples. As shown in Figure S1F, we can see that there is a large intersection of differentially expressed LncRNAs between five subtypes and all tumor samples.

3.2 | Differential expression of LncRNA copy number in melanoma subtype

The results of WGCNA co-expression algorithm mining are shown in Figure 2A. To ensure that the network is scale-free, we choose $\beta = 3$ (Figure 2B,C). Cluster analysis was conducted on the modules, and 39 modules were obtained (Figure 2D). Gene and LncRNA statistics in each module are shown in Table 3 and Figure 2E (wgcna.all.lnc.count.txt). We selected the intersection of the top 15 modules with the largest number of LncRNAs in the module and the top 15 modules with the largest LncRNA enrichment factor. There are four modules: dark green, midnight-blue, dark red, and tan; afterward, the analysis of the functions of these modules shows that all the four modules (module.enrich.txt) are enriched to 8, 4, 11, and 8 Pathways, respectively (Figure 2F).

In addition, we used GISTIC 2.0 software to analyze the copy number data of 366 melanoma cases downloaded from TCGA, the copy number variation of each gene such as all_thresholded.by_genes.txt. Its distribution in the genome is shown in Figure 2G. It can be seen that the proportion of copy amplification is similar to that of copy deletion, with the largest proportion of deletion on chromosomes 9 and 10, and the largest proportion of amplification on chromosomes 6 and 7. Furthermore, we calculated the correlation between LncRNA expression profile and copy number, as shown in Figure 2H, and it can be seen that the expression of LncRNA and copy number showed an overall positive correlation trend, and their distribution was increased than that of random distribution ($P < 1e{-}16$). There are many LncRNAs with an increased number of copies or deletions, and the copy deletion of LncRNAs is more frequent than the copy amplification region (Figure 2I), which suggests that LncRNA copy deletion may be related to the occurrence and development of melanoma. To further observe the relationship between LncRNA expression and copy number, we selected 45 LncRNAs (P30.lnc.cnv.txt) with a copy number ratio of more than 5% in each sample. The expression differences of each LncRNA in copy amplification samples or copy deletion and copy normal samples were analyzed. We selected at least 10 samples with an expression greater than 0 in each group, and finally 29 LncRNAs (Figure 2J) were obtained. It can be seen that the expression of 13 LncRNAs in copy amplification samples was higher than that in normal copy samples, and the expression of one LncRNA in copy deletion samples was lower than that in normal samples, which suggests that the change of LncRNA copy number is closely related to the expression of LncRNA.
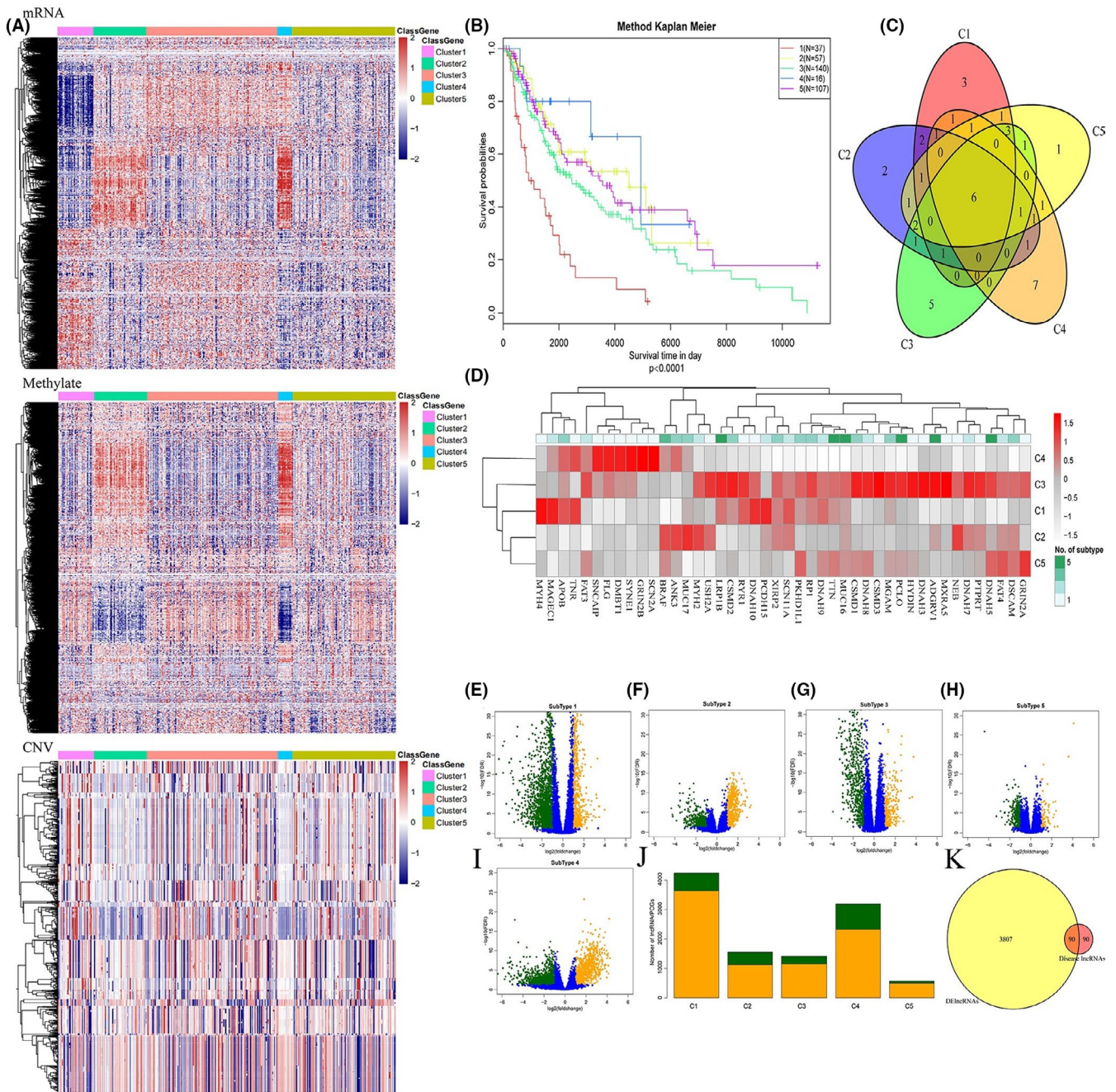
FIGURE 1 Multiomics screening of LncRNA differences in melanoma subtypes. A, Multigroup cluster analysis on mRNA, methylation data, and CNV all have significant differences in the three distribution levels among each subtype. B, KM survival curves of five melanoma subtypes. C, Wayne diagram of the upper 20 genes with highest mutation frequencies in each subtype. D, The mutation frequency heat maps of the top 20 genes with the highest mutation in each subtype in various samples. E-I, Differences among the five subtypes of LncRNA volcano maps, with orange indicating upregulation and green downregulation. J, Distribution of different lncRNAs and coding genes within each group with orange indicating genes and green indicating lncRNAs. K, Venn diagram of lncRNAs differentially associated with disease-related lncRNAs

3.3 | Screening LncRNAs associated with prognosis of melanoma

We analyzed the copy number of different LncRNAs in each subtype, and a total of 108 LncRNAs (sig.lncRNA.txt) were obtained, and the relationship between these 108 LncRNAs and total survival time

was analyzed respectively, as shown in lst.lnc.cox.txt. The LncRNAs with univariate cox and KM P values less than .05 were selected, and 11 LncRNAs were finally obtained, which were positively correlated with poor prognosis, as shown in Table 4.

Afterward, we analyzed their efficacy in prognosis classification according to the expression levels of the 11 LncRNAs that

TABLE 2 Differences in statistics for each subtype

Type	C1	C2	C3	C4	C5
PCG_Down	2838	510	784	1089	386
PCG_Up	793	609	363	1231	102
PCG_All	3631	1119	1147	2320	488
Lnc_Down	2124	413	602	796	287
Lnc_Up	607	433	268	870	77
Lnc_All	2731	846	870	1666	364

impacted the poor prognosis in each sample and plotted the ROC curve (Figure 3A). It can be seen that the average AUC area of these 11 LncRNAs was about 0.61. We screened six LncRNAs with an AUC greater than the mean. Multivariate survival analysis was used to observe whether these LncRNAs were independent prognostic factors. Afterward, four LncRNAs (Table 5) were screened, and according to the multivariate regression model of four LncRNAs (RiskScore = 0.09 * ENSG00000215196 + −0.11 * ENSG00000233834 + −0.18 * ENSG00000215769 + 0.43 * ENSG00000267014), we calculated the risk scores of each sample. According to the risk scores, the samples were divided into high-risk and low-risk groups. Simultaneously, the samples were divided into high- and low-expression groups according to the median, and the KM curve (Figure 3A) was made. It can be seen that the prognosis of high-risk samples was worse than that of low-risk samples.

To observe the function of these four LncRNAs, we used the gene expression profile to enrich and analyze the KEGG Pathway and GO Term of each sample by ssGSEA, and further screened the top 20 KEGG Pathways and GO Term with the highest correlation with the sample risk score (Figure 3B). To verify the effect of these four CNV-related LncRNAs on prognosis, we downloaded the standardized clinical data of GSE65904 data from GEO, which contains 214 samples. We extracted the expression profiles of these four LncRNAs, and ENSG00000233834 and ENSG00000267014 were not detected. Finally, two LncRNAs (*BASP1-AS1* and *ARHGAP27P1*) were detected the expression profiles. We further analyzed the relationship between the expression levels of these two LncRNAs and the prognosis. According to the median expression levels of these two LncRNAs, patients were divided into high-expression and low-expression groups to analyze their prognosis, and the KM curve (Figure 3C,D) shows that both LncRNAs have prognosis differences, which is similar to the training set. Afterward, we used multivariate Cox regression to establish a risk prediction model and calculated the prognostic risk scores of each sample. Furthermore, we divided the high-risk group and the low-risk group according to the median of the risk score of the sample. The difference in the prognosis of the high-risk group and the low-risk group was analyzed as shown in Figure 3E, and it can be seen that the prognosis of the high-risk group was more negative than that of the low-risk group ($P < .01$).

3.4 | *BASP1-AS1* depressed cell apoptosis via BCL-2

As shown in Figure 4A, *BASP1-AS1* was located at chromosome 5 with a conversed orientation of *BASP1*. Subcellular fractionation demonstrated the nucleus localization of *BASP1-AS1*, which hinted that *BASP1-AS1* might participate in the transcription process (Figure 4B). Next, to determine whether *BASP1-AS1* regulated melanoma progression, the expression of *BASP1-AS1* was detected in tumors and adjacent tissues by qRT-PCR. The result showed that *BASP1-AS1* was upregulated in tumors compared with adjacent tissues (Figure 4C). Furthermore, the result of qRT-PCR also validated the expression pattern of *BASP1-AS1* in different kinds of melanoma cells. A375 and SK-MEL-2 displayed the highest *BASP1-AS1* expression, so we decided to use A375 and SK-MEL-2 for further experiments (Figure 4D). To further investigate the effect of *BASP1-AS1* on melanoma progression, we constructed a recombinant pcDNA3.1 plasmid to overexpress *BASP1-AS1* and siRNA constructs to knockdown *BASP1-AS1*. Afterward, transfection efficiency was measured by a qRT-PCR assay (Figure 4E,F), and the top-10 *BASP1-AS1* positive correlated genes were determined using TCGA co-expression network analysis (Figure 4G). Among them, as the key regulator of apoptosis process, BCL-2 aroused our great interest (Figure 4H). By using qRT-PCR and western blot assays, we found that both BCL-2 mRNA and protein levels decreased after *BASP1-AS1* knockdown (Figure 4I). Moreover, cell apoptosis rate also increased after si *BASP1-AS1* transfection (Figure 4J). Furthermore, the expression of apoptosis-related proteins also increased in the *BASP1-AS1* knockdown group, which was determined using Tunel assays (Figure 4K). Taken together, *BASP1-AS1* inhibited cell apoptosis by upregulating BCL-2 during melanoma progression.

3.5 | Knockdown of *BASP1-AS1* suppressed cell proliferation, migration, and invasion in vitro and in vivo

Several experiments were performed to investigate further the effect of *BASP1-AS1* on cell function, such as cell proliferation and invasion. Two different *BASP1-AS1* target siRNA were transfected in A375 and SK-MEL-2 cell lines. Colony formation assays detected the proliferation of cells (Figure 5A); besides, the migration and
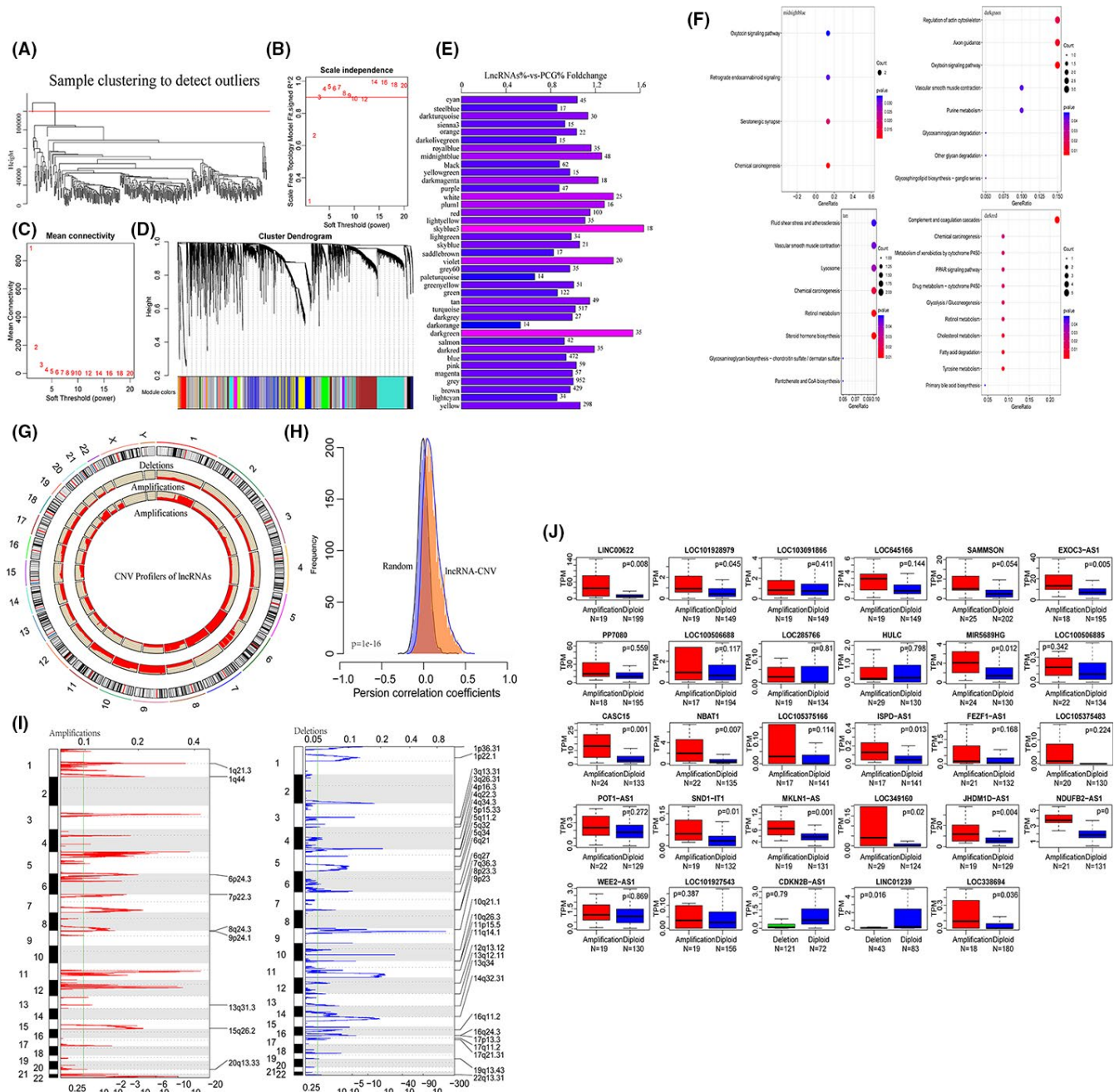
FIGURE 2 Differential expression of LncRNA copy number in melanoma subtype. A, Sample cluster analysis. B, C, Analysis of network topology for various soft-thresholding powers. D, Gene dendrogram and module colors. E, Relative multiple histograms of lncRNA ratios to PCG in 39 modules. The value on the right is the number of statistically significant lncRNA modules. The horizontal axis indicates the multiple of the ratio of lncRNA to PCG in the module and the vertical axis is the module. F, Results of KEGG enrichment of upper dark green, midnight blue, dark red, and tan modules. G, LncRNA copy deletion and copy amplification ratio distributions in the genome. H, Distribution of lncRNA expression and CNV, with light blue indicating the distribution under random conditions and light red the distribution under actual conditions. A *t*-test was used to test for statistical significance between the two distributions. I, LncRNAs located in the focal CNV peaks are SKCM-related. False-discovery rates (*q* values) and scores from GISTIC 2.0 for alterations (*x* axis) are plotted against genome positions (*y* axis). Dotted lines indicate the centromeres. The deletions (right, blue) and amplifications (left, red) of lncRNA genes are also shown. The green line represents the 0.25 *q* value cutoff point that determines signficance. J, Differences in expression of 29 lncRNAs in samples with copy amplification or deletion and samples copying normal

invasion ability of melanoma cells were also inhibited by siRNA *BASP1-AS1* (Figure 5B,C). To validate whether or not *BASP1-AS1* regulates cell proliferation in vivo, a tumor formation assay was performed. As shown in Figure 5D, the siRNA *BASP1-AS1* suppressed the volume and weight of the tumor, indicating *BASP1-AS1* increased cell proliferation during melanoma progression.

TABLE 3 Gene and LncRNA statistics for each module

Module	All	Lnc	PCG	Fc
Yellow	679	298	381	1.063743
Lightcyan	88	34	54	0.856309
Brown	1028	429	599	0.974038
Grey	2245	952	1293	1.001345
Magenta	135	57	78	0.993861
Pink	137	59	78	1.028733
Blue	1156	472	684	0.938494
Darkred	75	35	40	1.190018
Salmon	104	42	62	0.921304
Darkgreen	66	35	31	1.535507
Darkorange	50	14	36	0.528897
Darkgrey	64	27	37	0.992447
Turquoise	1206	517	689	1.020509
Tan	107	49	58	1.148983
Green	315	122	193	0.859702
Greenyellow	120	51	69	1.005233
Paleturquoise	43	14	29	0.656562
grey60	84	35	49	0.971443
Violet	40	20	20	1.360021
Saddlebrown	45	17	28	0.825727
Skyblue	48	21	27	1.057794
Lightgreen	81	34	47	0.983845
skyblue3	33	18	15	1.632025
Lightyellow	78	35	43	1.106993
Red	218	100	118	1.15256
plum1	33	16	17	1.280019
White	50	25	25	1.360021
Purple	120	47	73	0.87563
Dark magenta	38	18	20	1.224018
Yellow green	36	15	21	0.971443
Black	158	62	96	0.878347
Midnight blue	100	48	52	1.255404
Royal blue	76	35	41	1.160993
Dark olivegreen	39	15	24	0.850013
Orange	51	22	29	1.03174
sienna3	37	15	22	0.927287
Dark turquoise	66	30	36	1.13335
Steel blue	44	17	27	0.856309
Cyan	104	45	59	1.037304

3.6 | *BASP1-AS1* regulated melanoma progression by targeting Notch signaling and downstream molecules

To further clarify the specific molecular mechanism of *BASP1-AS1* during melanoma progression, next-generation sequencing was

TABLE 4 Significant difference in prognosis of LncRNAs

| LncRNA	P value	HR	Low 95% CI	High 95% CI	logrank P value	Symbol	CNV rate	PCC	DECount
ENSG00000237940	.013276016	0.796858334	0.665770694	0.953756615	0.006011162	LINC01238	0.013586957	0.189431043	2
ENSG00000215196	.031335812	1.089219997	1.007683925	1.177353507	0.009139403	BASP1-AS1	0.043478261	0.182492469	1
ENSG00000233834	.014418621	0.862509762	0.766136331	0.971006149	0.003917892	LOC100506098	0.038043478	0.034587399	3
ENSG00000231721	.007164485	0.941435298	0.900922721	0.98376964	2.63E-05	LINC-PINT	0.046195652	0.229773032	1
ENSG00000233038	.002598425	0.861739027	0.782201276	0.949364535	2.60E-05	LOC100506585	0.043478261	0.027399439	2
ENSG00000245149	.04834326	0.837246759	0.701889315	0.998707518	0.016677472	RNF139-AS1	0.038043478	0.229667038	1
ENSG00000251562	.03651981	0.993719595	0.987868837	0.998605005	0.0090103	MALAT1	0.024456522	0.238891561	2
ENSG00000247774	.003362667	0.972183278	0.954024326	0.990687867	0.001251299	PCED1B-AS1	0.013586957	0.055782299	3
ENSG00000251301	.031697284	0.862427003	0.753489531	0.987114358	6.16E-06	LINC02384	0.027173913	0.00888111	3
ENSG00000215769	.001103543	0.804433283	0.705856214	0.916777234	0.000428786	ARHGAP27P1	0.016304348	0.087162131	2
ENSG00000267014	.048605387	1.616658748	1.002945144	2.605910727	0.040794591	LINC01532	0.013586957	0.105952794	1
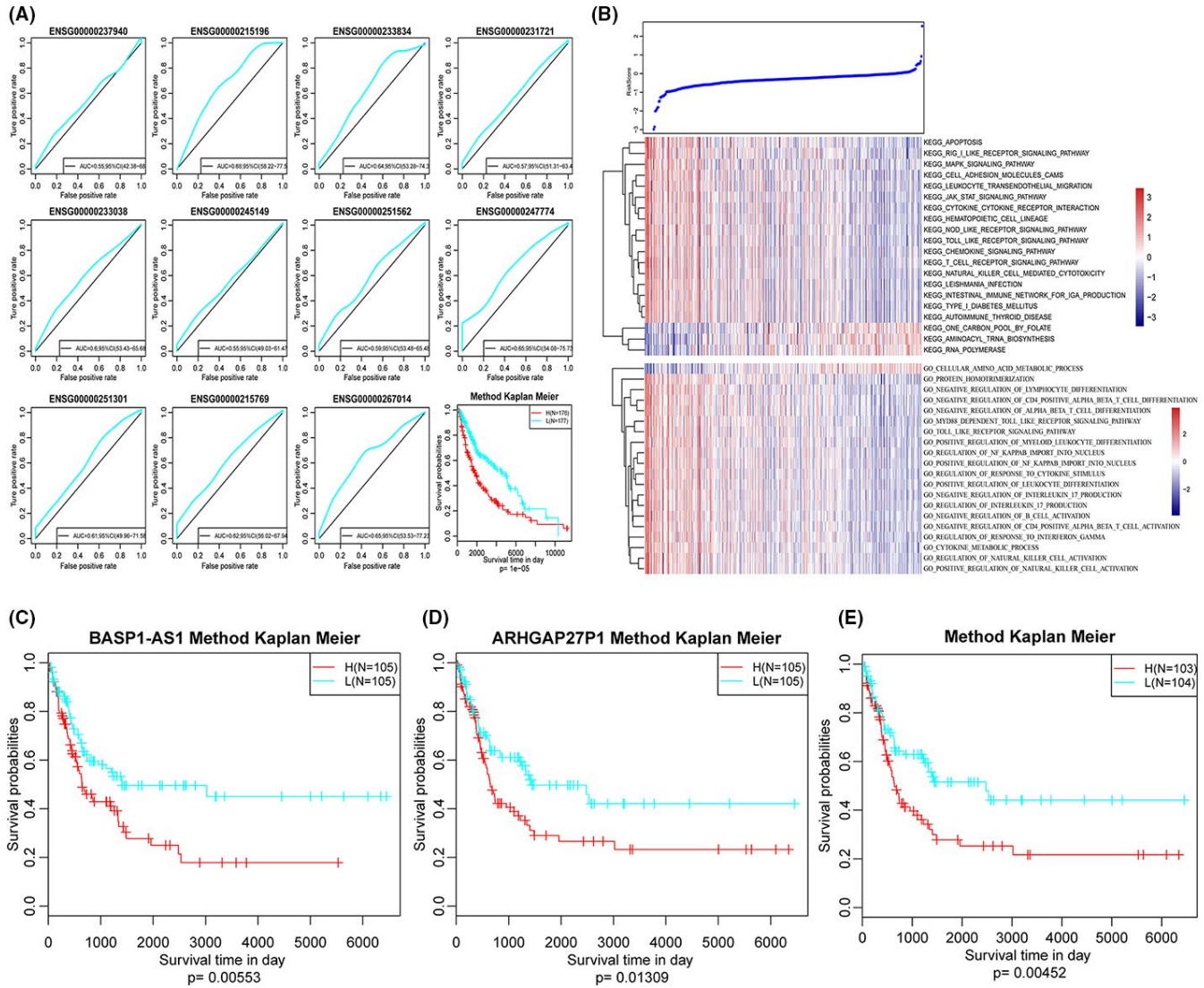
FIGURE 3 Screening LncRNAs associated with prognosis of melanoma. A, ROC curves of 11 LncRNAs with significant prognosis potential and prognostic differences as indicted in KM curves in four high- and low-risk groups of LncRNA multifactor models. B, Risk scores of the most relevant top 20 KEGG and GO pathway heat maps. C, KM curves of LncRNA BASP1-AS1. D, KM curves of LncRNA ARHGAP27P1. E, Two LncRNA multivariate regression models predicted prognostic differences in the KM curves of these samples

TABLE 5 Four prognostic independent CNV-related lncRNA molecules

lncRNA	Symbol	Exp(coef)	Lower 0.95	Upper 0.95	z	Pr(>|z|)
ENSG00000215196	BASP1-AS1	1.090817357	1.009935497	1.178176734	2.211481495	0.027002512
ENSG00000233834	LOC100506098	0.89881841	0.795600195	1.015427773	−1.713973181	0.086533651
ENSG00000215769	ARHGAP27P1	0.839351815	0.733129039	0.960965167	−2.536722134	0.011189573
ENSG00000267014	LINC01532	1.530696045	1.001950489	2.338469223	1.968976251	0.048955818

performed to demonstrate the differentially expressed genes after BASP1-AS1 knockdown (Figure 6A,B). As shown in Figure 6C, a total of 1371 genes were upregulated and 1031 genes were downregulated after BASP1-AS1 knockdown. Among them, the expression NOTCH3 was suppressed by si BASP1-AS1 transfection, suggesting its function as a key regulator of the Notch signaling pathway (Figure 6D). Furthermore, GSEA analysis of RNA-Seq data was used to demonstrate that the BASP1-AS1 knockdown regulated MYC

target genes (Figure 6E). Therefore, we supposed that BASP1-AS1 regulated the expression of NOTCH3, thereby regulating the downstream molecular targets, including c-MYC. Afterward, qRT-PCR and western blot assays were performed after si BASP-AS1 transfection to validate our hypothesis. The result demonstrated that both NOTCH3 and c-MYC were downregulated in the siRNA BASP1-AS1 group (Figure 6F,G). We also detected several c-MYC target oncogenes, such as PCNA, CDK4, MCM2, and PSMD1, using qRT-PCR

(Figure 6H,I). The result showed that depletion of NOTCH3 inhibited the expression of PCNA, CDK4, MCM2, and PSMD1, which can be abrogated by *BASP1-AS1* overexpression, hinting that *BASP1-AS1* regulated c-MYC and downstream molecules by NOTCH3.

3.7 | *BASP1-AS1* regulate NOTCH3 transcription by interacting with YBX1

Bioinformatics analysis was performed based on the catRAPID and RBPDB database to validate whether *BASP1-AS1* participates in the NOTCH3 transcription process. Both catRAPID and RBPDB databases anticipated that *BASP1-AS1* interacted with transcription factor Y-box binding protein 1 (YBX1) (Figure 7A). Moreover, the data from the TCGA database suggested that YBX1 was upregulated in melanoma (Figure 7B). These results were further validated by qRT-PCR in clinical sample tissues (Figure 7C). Interestingly, the result of qRT-PCR showed that *BASP1-AS1* does not affect YBX1 expression (Figure 7D). Nevertheless, the interaction between *BASP1-AS1* and YBX1 was also validated by RIP and RNA-pulldown assays, suggesting that *BASP1-AS1* may function as a regulator during the genes transcription process (Figure 7E,F).

In addition, CHIP assays were performed using NOTCH3 promoter-specific primers to validate whether or not *BASP1-AS1* and YBX1 participated in the transcription process of NOTCH3. The result demonstrated that YBX1 was enriched in the promoter of NOTCH3, and that the *BASP1-AS1* knockdown could suppress the combination (Figure 7G,H). We next constructed YBX1 targeting siRNA and examined the knockdown efficiency (Figure 7I). In addition, siRNA YBX1 decreased NOTCH3 expression, and *BASP1-AS1* did not affect NOTCH3 after YBX1 knockdown (Figure 7J,K).

We also transfected YBX1 target siRNA in A375 and SK-MEL-2 cell lines. Colony formation assays detected the proliferation of cells (Figure 8A); besides, the migration and invasion ability of melanoma cells were also inhibited by siRNA YBX1 (Figure 8B,C). The results indicate YBX1 increased cell proliferation and invasion during melanoma progression. We detected several NOTCH3 target molecules such as Hes1 and Hey1/2, and the western blot result confirmed that *BASP1-AS1* knockdown could decrease these proteins' expression levels (Figure 9A). Taken together, as shown in Figure 9B, our study suggested that *BASP1-AS1* was essential for YBX1-mediated NOTCH3 expression. *BASP1-AS1* interacted with YBX1 and recruited it to the promoter of NOTCH3, initiating its transcription process. The activation of Notch signaling then resulted in the transcription of multiple oncogenes, including c-MYC, PCNA, and CDK4, which contributed to melanoma progression.

4 | DISCUSSION

The development of melanoma is an extremely complex process. The abnormal expression of LncRNA in tumor tissues and cells is considered a promising biomarker for the diagnosis and prognosis of various cancers.[26] So far, there are few studies on LncRNAs-CNV in melanoma.
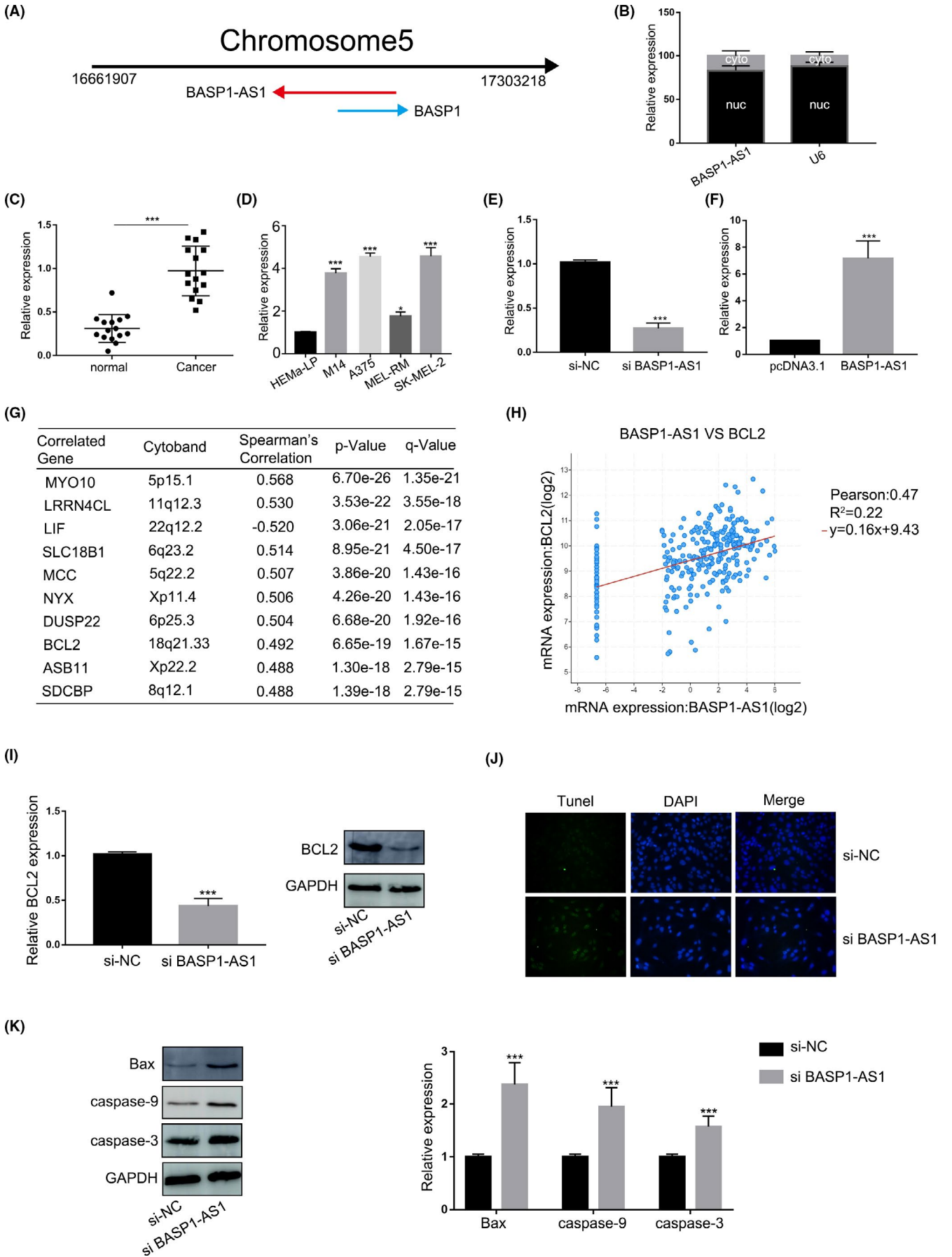
In this study, we used prognostic-related coding genes, CNV, and methylation sites, and selected 366 samples shared by the three omics to conduct a multigroup clustering analysis and constructed a prognostic model of four genes (*BASP1-AS1*, *LOC100506098*, *ARHGAP27P1*, and *LINC01532*) in the TCGA cohort, which was verified by GSE65904. Survival analysis showed that functional LncRNAs-CNV might be a candidate prognostic biomarker for clinical application. We found that *BASP1-AS1* is a novel LncRNA and is associated with the prognosis of melanoma. Compared with normal cells and tissues, *BASP1-AS1* was upregulated in melanoma cells and tissues. High expression of *BASP1-AS1* is associated with the proliferation, invasion, and migration of melanoma cells, resulting in the rapid growth of tumors in vivo. Knockdown of *BASP1-AS1* can inhibit the proliferation, tumor growth, and melanoma cell invasion and migration in vivo.

Furthermore, we found that BCL-2 is a key regulator of apoptosis using the TCGA co-expression network analysis. In addition, the qRT-PCR and western blot revealed that the mRNA and protein levels of BCL-2 decreased after *BASP1-AS1* gene knockdown. After transfection of siRNA *BASP1-AS1*, both the apoptosis rate and the expression of apoptosis-related proteins increased in the *BASP1-AS1* knockdown group. Those results suggest that *BASP1-AS1* inhibits apoptosis in melanoma progression by upregulating BCL-2. Therefore, we concluded that *BASP1-AS1* is a carcinogenic LncRNA in melanoma.

Despite our results, *BASP1-AS1* remains as an undefined LncRNA. At present, only *BASP1-AS1* regulates *BASP1* in hNPCs and plays a crucial role in neuronal differentiation.[19] The importance of *BASP1-AS1* in the progression and prognosis of melanoma is still unclear. In this study, we used the subcellular stratification technique to find that *BASP1-AS1* was localized in the nucleus, suggesting that *BASP1-AS1* may be involved in the transcription process. We used next-generation sequencing technology to find differentially expressed genes after *BASP1-AS1* knockout and found that the expression of NOTCH3 was inhibited. It is suggested that *BASP1-AS1* regulates NOTCH3 to promote the proliferation and migration of melanoma cells, leading to tumor growth.

Next, we used RNA-Seq data for GSEA analysis and found that the downregulation of *BASP1-AS1* regulated MYC target genes.

FIGURE 4 BASP1-AS1 inhibited cell apoptosis by upregulating BCL-2. A, Schematic diagram of BASP1-AS1 in chromosome. B, The localization of BASP1-AS1 was measured in cells by cytoplasmic and nuclear mRNA fractionation experiment. C, The expression of BASP1-AS1 was measured by qRT-PCR in tissues. D, The expression of BASP1-AS1 was measured by qRT-PCR in cells. E, F, The efficiency of si BASP1-AS1 and pcDNA3.1 BASP1-AS1 was validated by qRT-PCR. G, BASP1-AS1 correlated genes were analyzed by TCGA database. H, The correlation between BASP1-AS1 and BCL-2 in TCGA. I, The expression of BCL-2 was detected by qRT-PCR and western blot after si BASP1-AS1 transfection. J, The apoptotic rate of A375 cells was measured by Tunel assays. K, The expression of apoptosis-related proteins was measured by western blot
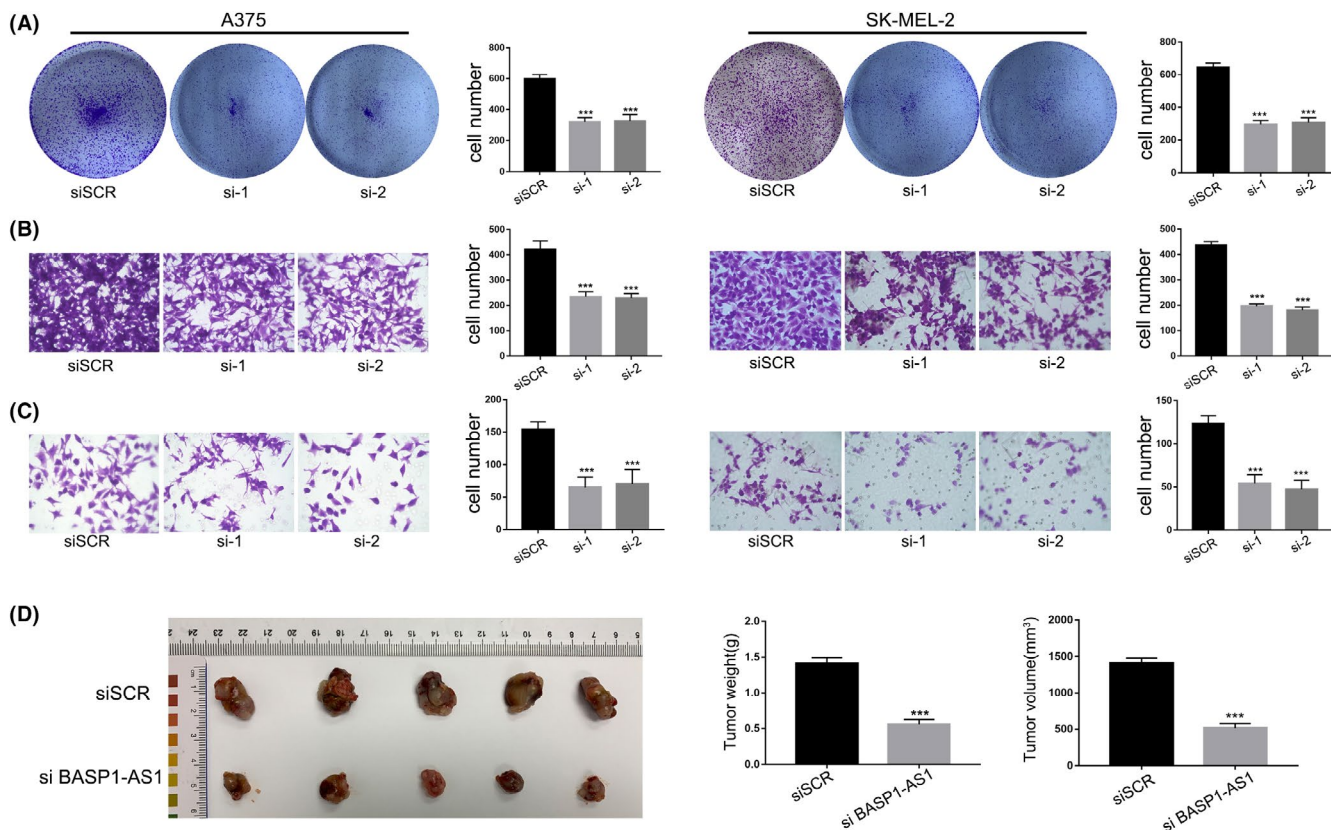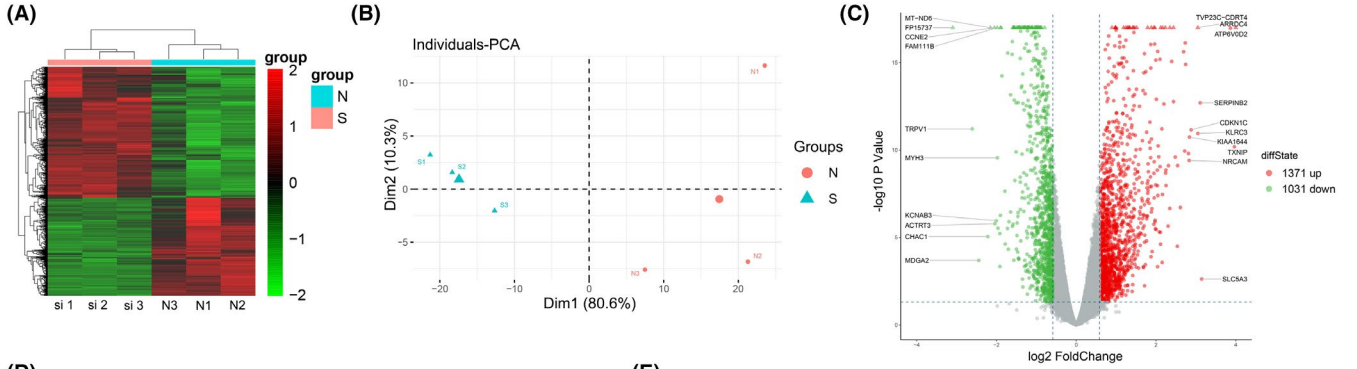
(A)

Chromosome5

16661907 ←BASP1-AS1 17303218

→ BASP1

(B)

(C)

(D)

(E)

(F)

(G)

Correlated Gene	Cytoband	Spearman's Correlation	p-Value	q-Value
MYO10	5p15.1	0.568	6.70e-26	1.35e-21
LRRN4CL	11q12.3	0.530	3.53e-22	3.55e-18
LIF	22q12.2	-0.520	3.06e-21	2.05e-17
SLC18B1	6q23.2	0.514	8.95e-21	4.50e-17
MCC	5q22.2	0.507	3.86e-20	1.43e-16
NYX	Xp11.4	0.506	4.26e-20	1.43e-16
DUSP22	6p25.3	0.504	6.68e-20	1.92e-16
BCL2	18q21.33	0.492	6.65e-19	1.67e-15
ASB11	Xp22.2	0.488	1.30e-18	2.79e-15
SDCBP	8q12.1	0.488	1.39e-18	2.79e-15

(H)

BASP1-AS1 VS BCL2

Pearson:0.47
R^2=0.22
y=0.16x+9.43

(I)

(J)

(K)

FIGURE 5 Downregulating of BASP1-AS1 decreased cell proliferation and invasion in vitro and in vivo. A, The effect of BASP1-AS1 on cell proliferation was detected by colony formation assays after transfection in vitro. B, C, Cell migration and invasion assays were used to measure the effect of BASP1-AS1 on cell invasion. D, A subcutaneous tumor formation experiment was used to measure the effect of BASP1-AS1 on cell proliferation ability in vivo

Therefore, we speculated that *BASP1-AS1* regulated c-MYC and its downstream molecules through NOTCH3, and qRT-PCR and western blot confirmed our inference. Recent studies have shown that the Notch proteins can be carcinogenic or tumor suppressors, depending on the tissue and cell environment. Therefore, the Notch pathway represents an important target for the design of therapeutic agents to treat various types of cancer.[27] The most typical carcinogenic function of Notch in human cancer is to open the gene expression program for the growth increase of supporting cells and focus on c-MYC to increase the expression of Notch.[28-30] NOTCH3 is upregulated most obviously in melanoma-initiated metastatic cell lines, and NOTCH3 interacts with LEC to induce the conversion of melanoma cells to 3D growth.[31] NOTCH3 can reduce the invasion and diffusion of melanoma, and it inhibits the growth, colony formation, and microtubule formation of melanoma in vitro and in vivo.[32] c-MYC is a proto-oncogene with clear characteristics, which can induce cell transformation and regulate programmed cell death. Overexpression of c-MYC promotes the development of melanoma.[23,24]
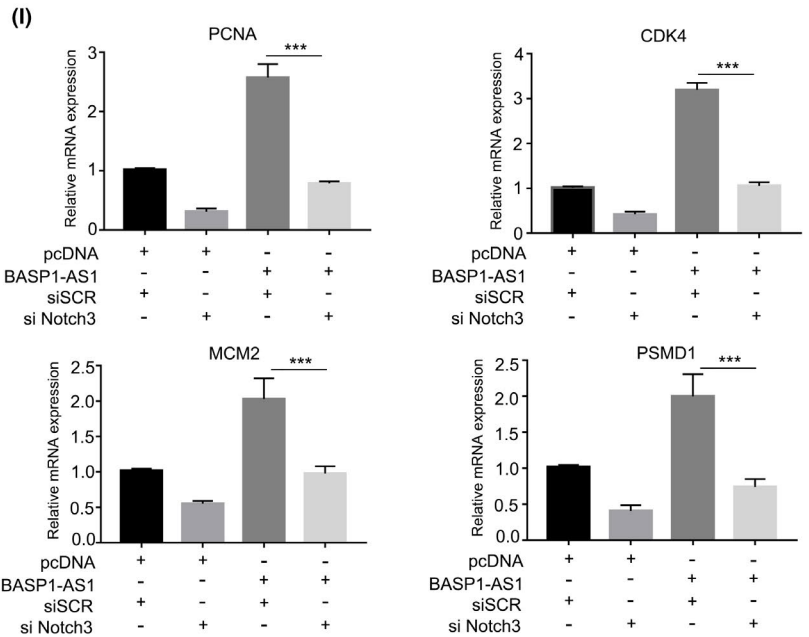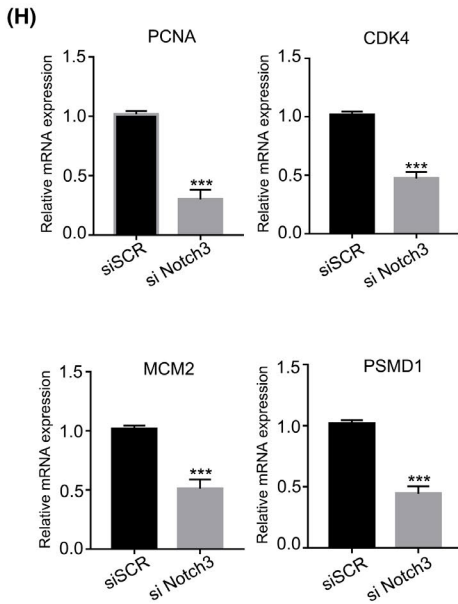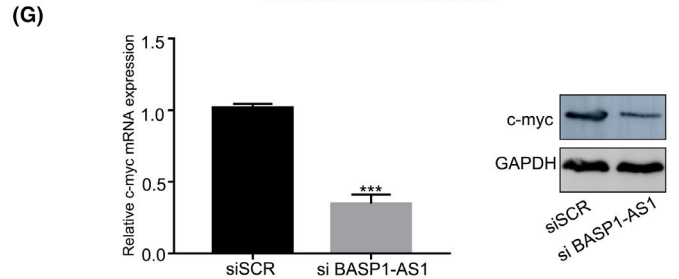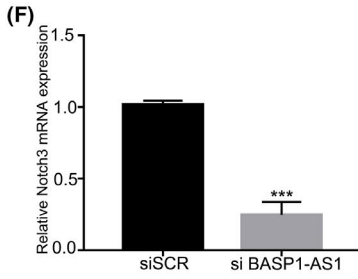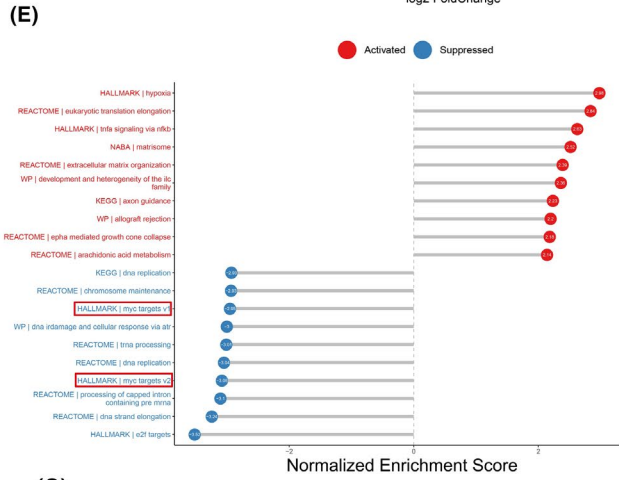
In melanoma, the regulatory mechanism of *BASP1-AS1* on NOTCH3 is still unclear. We determined the interaction between *BASP1-AS1* and YBX1 through bioinformatics analysis, qRT-PCR, western blot, RIP analysis, RNA pulldown, and CHIP profiling and recruited it to the promoter of NOTCH3 to initiate its transcription process. YBX1 is a DNA and RNA binding protein involved in various cellular processes, including transcription and translation regulation, pre-mRNA splicing, DNA repair, and mRNA packaging. Its abnormal expression is related to cancer proliferation in many tissues and may be a prognostic marker for poor prognosis and drug resistance in some cancers.[33,34] Studies have shown that a variety of LncRNAs interact with YBX1 to affect its transcription factor function. For example, LncRNA *DSCAM-AS1* interacts with YBX1 to promote cancer progression by forming a positive feedback loop that activates the FOXA1 transcription network.[21] LncRNA *HOXC-AS3* participates in

FIGURE 6 BASP1-AS1 regulated tumor progression by notch signaling pathway. A-C, The downstream genes of BASP1-AS1 were explored by next-generation sequencing. D, The top-15 downregulated genes after si BASP1-AS1 transfectio. E, GSEA analysis indicated a significant correlation between BASP1-AS1 and MYC-related gene signatures. F, G, The expression of Notch3 and c-myc was decreased after BASP1-AS1 transfection. H, The expression of PCNA, CDK4, MCM2 and PSMD1 decreased after si Notch3 transfection. I, The expression of PCNA, CDK4, MCM2 was detected by qRT-PCR after si Notch3 and BASP1-AS1 co-transfection

(A) — Heatmap with group legend (N, S), color scale from -2 to 2; columns labeled si 1, si 2, si 3, N3, N1, N2.

(B) Individuals-PCA. Dim2 (10.3%) vs Dim1 (80.6%). Groups: N (circle), S (triangle). Points labeled N1, N2, N3, S1, S2, S3.

(C) Volcano plot. -log10 P Value vs log2 FoldChange. diffState: 1371 up (red), 1031 down (green). Labeled genes: MT-ND6, FP15737, CCNE2, FAM111B, TRPV1, MYH3, KCNAB3, ACTRT3, CHAC1, MDGA2, TVP23C-CDRT4, ARRDC4, ATP6V0D2, SERPINB2, CDKN1C, KLRC3, KIAA1644, TXNIP, NRCAM, SLC5A3.

(D)

Gene symbol	Cytoband	logFC	p-Value	q-Value
TRPV1	Chr17	-2.60	6.23E-12	2.61E-10
MDGA2	Chr14	-2.44	2.03E-04	1.04E-03
CHAC1	Chr15	-2.21	9.01E-06	7.34E-05
CCNE2	Chr8	-2.05	5.29E-24	2.50E-21
ACTRT3	Chr3	-2.04	1.63E-06	1.75E-05
KCNAB3	Chr17	-2.00	1.11E-06	1.25E-05
FAM111B	Chr11	-1.98	1.41E-23	5.82E-21
MYH3	Chr17	-1.97	2.79E-10	8.18E-09
SLC23A3	Chr2	-1.96	2.97E-06	2.86E-05
E2F2	Chr1	-1.91	6.04E-06	5.21E-05
TIMM23B	Chr10	-1.91	4.61E-04	2.1E-03
NOTCH3	Chr19	-1.89	5.50E-07	6.79E-06
HSPA5	Chr9	-1.89	1.01E-66	1.24E-62
ZNF804A	Chr2	-1.88	3.39E-20	8.19E-18
NCOA5	Chr20	-1.86	5.74E-15	4.18E-13

(E) GeneSets vs Normalized Enrichment Score. Activated (red), Suppressed (blue). Gene sets include: HALLMARK | hypoxia, REACTOME | eukaryotic translation elongation, HALLMARK | tnfa signaling via nfkb, NABA | matrisome, REACTOME | extracellular matrix organization, WP | development and heterogenity of the ilc family, KEGG | axon guidance, WP | allograft rejection, REACTOME | epha mediated growth cone collapse, REACTOME | arachidonic acid metabolism, KEGG | dna replication, REACTOME | chromosome maintenance, HALLMARK | myc targets v1, WP | dna irdamage and cellular response via atr, REACTOME | trna processing, REACTOME | dna replication, HALLMARK | myc targets v2, REACTOME | processing of capped intron containing pre mrna, REACTOME | dna strand elongation, HALLMARK | e2f targets.

(F) Relative Notch3 mRNA expression: siSCR vs si BASP1-AS1 (***). Western blot: Notch3, GAPDH for siSCR, si BASP1-AS1.

(G) Relative c-myc mRNA expression: siSCR vs si BASP1-AS1 (***). Western blot: c-myc, GAPDH for siSCR, si BASP1-AS1.

(H) Relative mRNA expression for PCNA, CDK4, MCM2, PSMD1: siSCR vs si Notch3 (***).

(I) Relative mRNA expression for PCNA, CDK4, MCM2, PSMD1 with conditions pcDNA, BASP1-AS1, siSCR, si Notch3 (***).
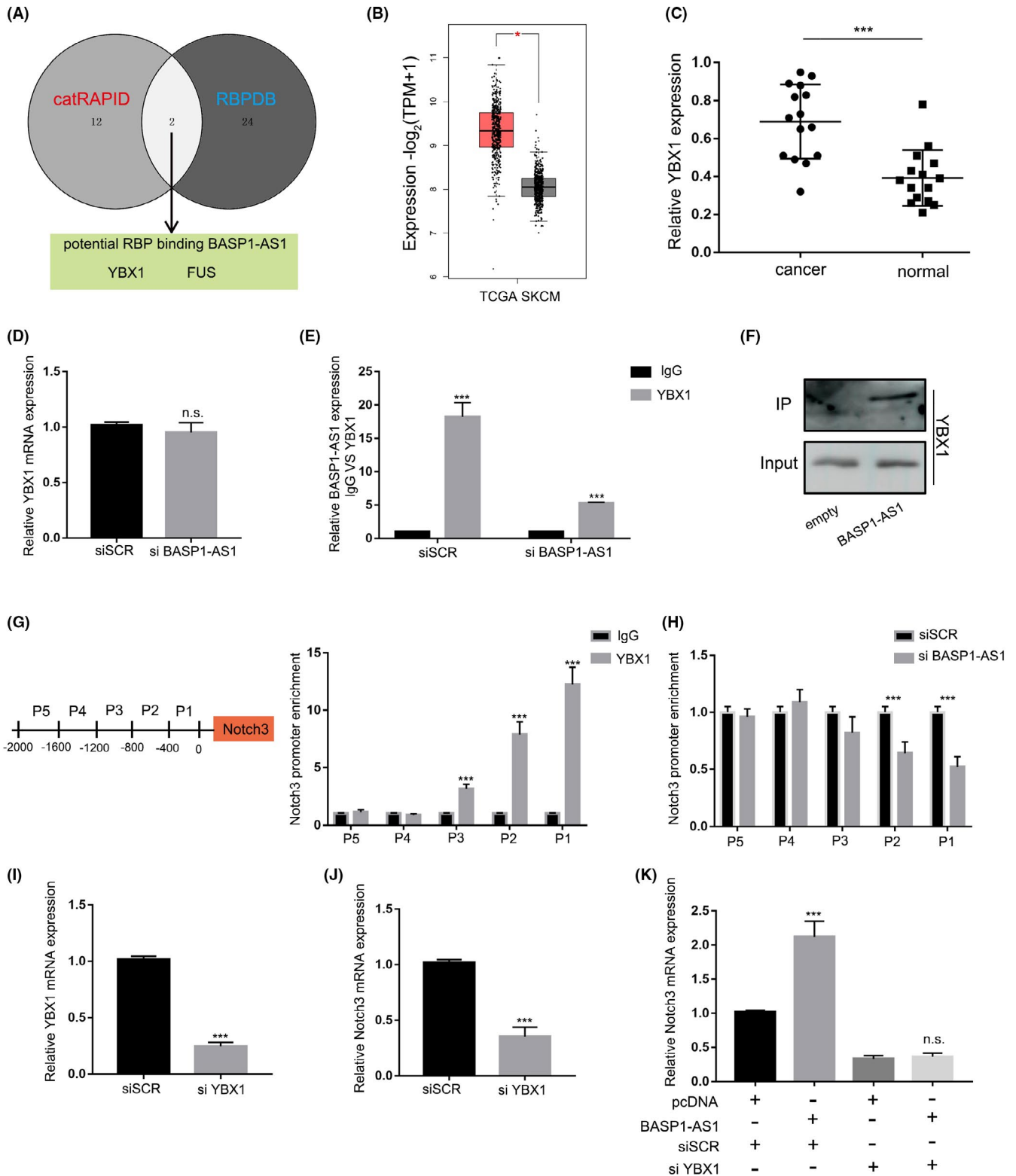
FIGURE 7 BASP1-AS1 interacted with YBX1 and regulated Notch3 transcription. A, The potential binding proteins of BASP1-AS1 was predicted by catRAPID and RBPDB database. B, The expression of BASP1-AS1 in SKCM was validated by TCGA database. C, The expression of BASP1-AS1 was measured by qRT-PCR. D, The effect of BASP1-AS1 on YBX1 was detected by qRT-PCR. E, The interaction between BASP1-AS1 and YBX1 was detected by RIP assays. F, The interaction was further confirmed by RNA-pulldown assays. G, H, The enrichment of YBX1 on the promoter of Notch3 was detected by ChIP assay. I, The efficiency of si YBX1 was validated by qRT-PCR. J, The effect of YBX1 on Notch3 expression was detected by qRT-PCR. K, The expression of Notch3 was detected by qRT-PCR after si YBX1 and BASP1-AS1 co-transfection
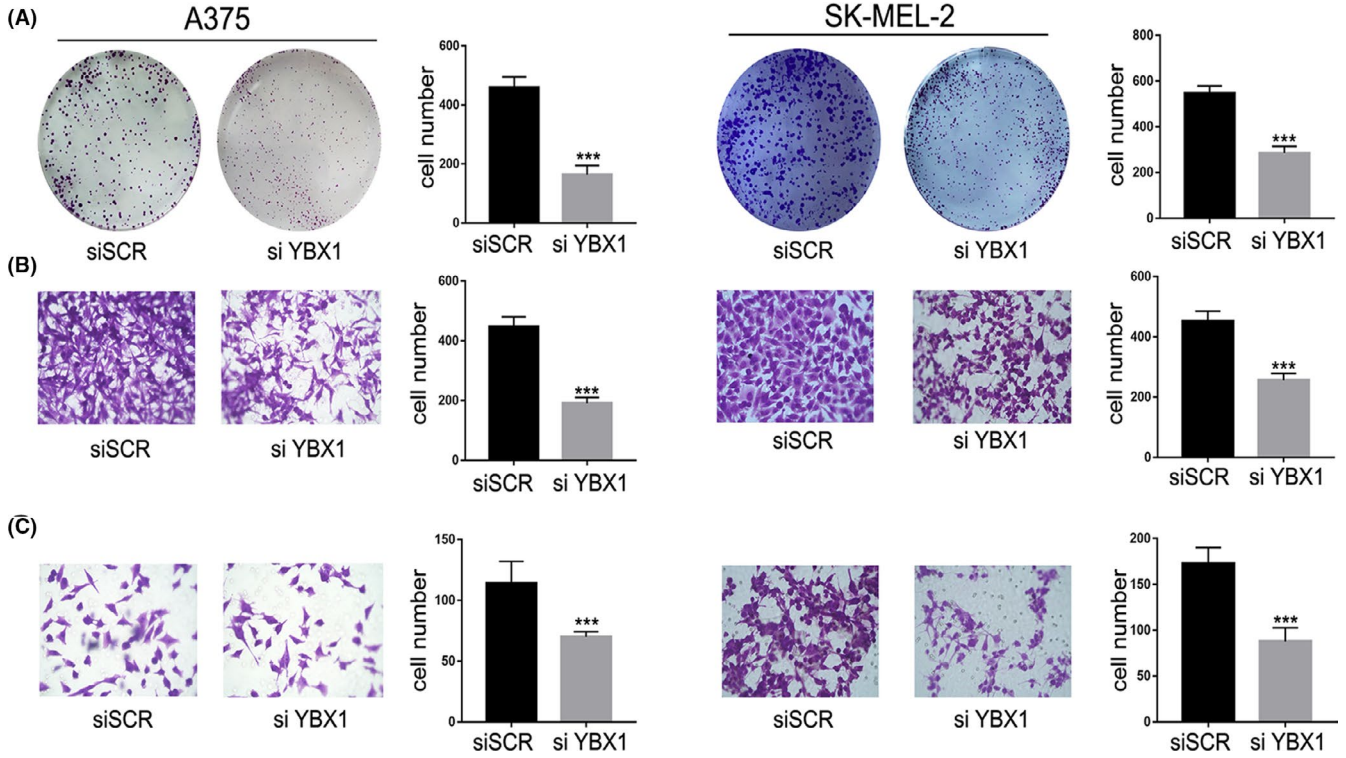
FIGURE 8 YBX1 knockdown significantly inhibited cell proliferation and invasion in vitro during melanoma progression. A, The effect of YBX1 on cell proliferation was detected by colony formation assays after transfection in vitro. B, C, Cell migration and invasion assays were used to measure the effect of YBX1 on cell invasion
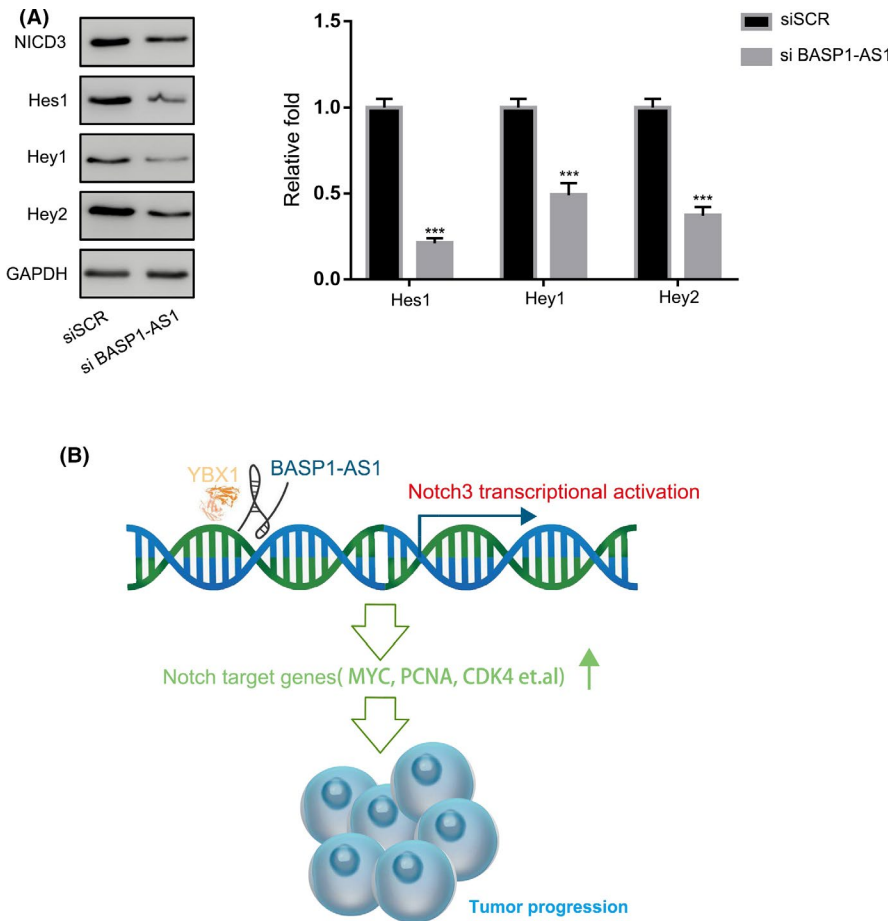

FIGURE 9 BASP1-AS1 regulated Notch signaling pathway target genes. A, The protein levels of Notch signaling pathway target genes were detected by western blot assays. B, Mechanism for the regulatory function of BASP1-AS1 in melanoma progression

tumorigenesis of gastric cancer through binding to YBX1 and transcriptional regulation of other genes.[22] LncRNA *LINC00312* induces migration and angiogenesis mimicry of lung adenocarcinoma by directly binding to YBX1.[35] Interestingly, qRT-PCR results showed that *BASP1-AS1* had no effect on the expression of YBX1, indicating that in addition to the BASP1-AS1/YBX1/NOTCH3 axis, there may be other regulatory mechanisms for target genes, and the detailed mechanism needs further study in the future.

In summary, we identified a new type of LncRNA *BASP1-AS1*, which can promote melanoma development both in vivo and in vitro. Detailed studies on the molecular mechanism showed that *BASP1-AS1* promoted the proliferation, invasion, and migration of melanoma cells by regulating YBX1. In addition, LncRNA *BASP1-AS1* is a poor prognostic indicator and a potential therapeutic target for melanoma.

ACKNOWLEDGEMENTS

DISCLOSURE

The authors have no conflict of interest.

ORCID

XiuHao Guan https://orcid.org/0000-0002-7308-7077

REFERENCES

1. Davis LE, Shalin SC, Tackett AJ. Current state of melanoma diagnosis and treatment. *Cancer Biol Ther.* 2019;20:1366-1379.
2. Topalian SL, Drake CG, Pardoll DM. Immune checkpoint blockade: a common denominator approach to cancer therapy. *Cancer Cell.* 2015;27:450-461.
3. George DD, Armenio VA, Katz SC. Combinatorial immunotherapy for melanoma. *Cancer Gene Ther.* 2017;24:141-147.
4. Turner N, Ware O, Bosenberg M. Genetics of metastasis: melanoma and other cancers. *Clin Exp Metastasis.* 2018;35:379-391.
5. Garbe C, Peris K, Hauschild A, et al. Diagnosis and treatment of melanoma. European consensus-based interdisciplinary guideline - Update 2016. *Eur J Cancer.* 2016;63:201-217.
6. Peng WX, Koirala P, Mo YY. LncRNA-mediated regulation of cell signaling in cancer. *Oncogene.* 2017;36:5661-5667.
7. Chandra Gupta S, Nandan TY. Potential of long non-coding RNAs in cancer patients: from biomarkers to therapeutic targets. *Int J Cancer.* 2017;140:1955-1967.
8. Batista PJ, Chang HY. Long noncoding RNAs: cellular address codes in development and disease. *Cell.* 2013;152:1298-1307.
9. Xu Y, Qiu M, Shen M, et al. The emerging regulatory roles of long non-coding RNAs implicated in cancer metabolism. *Mol Ther.* 2021;29(7):2209-2218.
10. Zou ZW, Ma C, Medoro L, et al. LncRNA ANRIL is up-regulated in nasopharyngeal carcinoma and promotes the cancer progression via increasing proliferation, reprograming cell glucose metabolism and inducing side-population stem-like cancer cells. *Oncotarget.* 2016;7:61741-61754.
11. Gao Y, Li Y, Niu X, et al. Identification and validation of prognostically relevant gene signature in melanoma. *Biomed Res Int.* 2020;2020:5323614.
12. Yepes S, Tucker MA, Koka H, et al. Using whole-exome sequencing and protein interaction networks to prioritize candidate genes for germline cutaneous melanoma susceptibility. *Sci Rep.* 2020;10:17198.
13. Ozsolak F, Milos PM. RNA sequencing: advances, challenges and opportunities. *Nat Rev Genet.* 2011;12:87-98.
14. Ramani V, Qiu R, Shendure J. High-throughput determination of RNA structure by proximity ligation. *Nat Biotechnol.* 2015;33:980-984.
15. Langfelder P, Horvath S. WGCNA: an R package for weighted correlation network analysis. *BMC Bioinformatics.* 2008;9:559.
16. Cheng Y, Liu C, Liu Y, et al. Immune microenvironment related competitive endogenous RNA network as powerful predictors for melanoma prognosis based on WGCNA analysis. *Front Oncol.* 2020;10:577072.
17. Cheng S, Li Z, Zhang W, et al. Identification of IL10RA by weighted correlation network analysis and in vitro validation of its association with prognosis of metastatic melanoma. *Front Cell Dev Biol.* 2020;8:630790.
18. Wang X, Chai Z, Li Y, et al. Identification of potential biomarkers for anti-PD-1 therapy in melanoma by weighted correlation network analysis. *Genes (Basel).* 2020;11:435.
19. Prajapati B, Fatima M, Fatma M, et al. Temporal transcriptome analysis of neuronal commitment reveals the preeminent role of the divergent lncRNA biotype and a critical candidate gene during differentiation. *Cell Death Discov.* 2020;6:28.
20. Suresh PS, Tsutsumi R, Venkatesh T. YBX1 at the crossroads of noncoding transcriptome, exosomal, and cytoplasmic granular signaling. *Eur J Cell Biol.* 2018;97:163-167.
21. Zhang Y, Huang YX, Wang DL, et al. LncRNA DSCAM-AS1 interacts with YBX1 to promote cancer progression by forming a positive feedback loop that activates FOXA1 transcription network. *Theranostics.* 2020;10:10823-10837.
22. Zhang E, He X, Zhang C, et al. A novel long noncoding RNA HOXC-AS3 mediates tumorigenesis of gastric cancer by binding to YBX1. *Genome Biol.* 2018;19:154.
23. Ravindran Menon D, Luo Y, Arcaroli JJ, et al. CDK1 interacts with Sox2 and promotes tumor initiation in human melanoma. *Cancer Res.* 2018;78:6561-6574.
24. Arasu UT, Deen AJ, Pasonen-Seppänen S, et al. HAS3-induced extracellular vesicles from melanoma cells stimulate IHH mediated c-Myc upregulation via the hedgehog signaling pathway in target cells. *Cell Mol Life Sci.* 2020;77:4093-4115.
25. Li YL, Gao YL, Niu XL, et al. Identification of subtype-specific metastasis-related genetic signatures in sarcoma. *Front Oncol.* 2020;10:544956.
26. Yu X, Zheng H, Tse G, Chan MT, Wu WK. Long non-coding RNAs in melanoma. *Cell Prolif.* 2018;51:e12457.
27. Nowell CS, Radtke F. Notch as a tumour suppressor. *Nat Rev Cancer.* 2017;17:145-159.
28. Aster JC, Pear WS, Blacklow SC. The varied roles of Notch in cancer. *Annu Rev Pathol.* 2017;12:245-275.
29. Palomero T, Lim WK, Odom DT, et al. NOTCH1 directly regulates c-MYC and activates a feed-forward-loop transcriptional network promoting leukemic cell growth. *Proc Natl Acad Sci USA.* 2006;103:18261-18266.
30. Sharma VM, Calvo JA, Draheim KM, et al. Notch1 contributes to mouse T-cell leukemia by directly inducing the expression of c-myc. *Mol Cell Biol.* 2006;26:8022-8031.
31. Pekkonen P, Alve S, Balistreri G, et al. Lymphatic endothelium stimulates melanoma metastasis and invasion via MMP14-dependent Notch3 and β1-integrin activation. *Elife.* 2018;7:e32490.
32. Hsu MY, Yang MH, Schnegg CI, Hwang S, Ryu B, Alani RM. Notch3 signaling-mediated melanoma-endothelial crosstalk regulates melanoma stem-like cell homeostasis and niche morphogenesis. *Lab Invest.* 2017;97:725-736.

33. Mordovkina D, Lyabin DN, Smolin EA, Sogorina EM, Ovchinnikov LP, Eliseeva I. Y-box binding proteins in mRNP assembly, translation, and stability control. *Biomolecules*. 2020;10:591.

34. Kuwano M, Shibata T, Watari K, Ono M. Oncogenic Y-box binding protein-1 as an effective therapeutic target in drug-resistant cancer. *Cancer Sci*. 2019;110:1536-1543.

35. Peng Z, Wang J, Shan B, et al. The long noncoding RNA LINC00312 induces lung adenocarcinoma migration and vasculogenic mimicry through directly binding YBX1. *Mol Cancer*. 2018;17:167.

SUPPORTING INFORMATION

Additional supporting information may be found in the online version of the article at the publisher's website.